IEEE Access
Multidisciplinary | Rapid Review | Open Access Journal

Received 26 November 2023, accepted 15 December 2023, date of publication 18 December 2023,
date of current version 26 December 2023.

Digital Object Identifier 10.1109/ACCESS.2023.3344534

RESEARCH ARTICLE

Adaptive Single Low-Light Image Enhancement by Fractional Stretching in Logarithmic Domain

THAWEESAK TRONGTIRAKUL[1], SOS S. AGAIAN[2], (Life Fellow, IEEE), AND SHIQIAN WU[3], (Senior Member, IEEE)

[1]Faculty of Industrial Education, Rajamangala University of Technology Phra Nakhon (RMUTP), Bangkok 10300, Thailand
[2]Graduate Center, The City University of New York (CUNY), New York, NY 10016, USA
[3]School of Information Science and Engineering, Wuhan University of Science and Technology (WUST), Wuhan 430081, China

Corresponding author: Thaweesak Trongtirakul (thaweesak.tr@rmutp.ac.th)

This work was partially supported in part by the Coordinating Center for Thai Government Science and Technology Scholarship Students (CSTS); and in part by the National Science and Technology Development Agency (NSTDA), Ministry of Higher Education, Science, Research, and Innovation, under Grant JRA-CO-2565-17450-TH.

ABSTRACT Low-light image enhancement is a challenging task that aims to improve the visibility and quality of images captured in dark environments. However, existing methods often introduce undesirable artifacts such as color distortion, halo effects, blocking artifacts, and noise amplification. In this paper, we propose a novel method that overcomes these limitations by using the logarithmic domain fractional stretching approach to estimate the reflectance component of the image based on the improved Retinex theory. Moreover, we apply a simple adaptive gamma correction algorithm to the *Lab* color-space to adjust the brightness and saturation of the image. Our method effectively reduces the impact of non-uniform illumination and produces enhanced images with natural and realistic colors. Extensive experiments across diverse public datasets substantiate the superiority of our method. In both subjective and objective evaluations, our approach outperforms state-of-the-art methods.

INDEX TERMS Retinex, image enhancement, logarithmic transformation, low-light image, fractional stretching functions, non-uniform illumination.

I. INTRODUCTION

Capturing images in low-light conditions, which include scenarios like indoors, nighttime scenes, and overcast weather, introduces substantial challenges, notably:

(1) Loss of Image Information: Insufficient illumination diminishes image quality and compromises visual perception, resulting in low-contrast images, reduced visible details, and inadequate lighting. These factors present formidable challenges for image-based analysis systems.

(2) Localized Exposure and Color Issues: Uneven illumination or non-uniform exposure can induce underexposure, overexposure, or color distortion in specific local regions of the output image. This challenge is particularly pronounced in dynamic scenarios such as fast-paced aerial scenes and streetscapes with varying illuminations, necessitating real-time processing and robust feature extraction.

Addressing these challenges is critical, given that images interpret a clear distinction between bright and dark regions and that diverse colors offer richer details about the scene. Such enhanced images are pivotal in numerous computer vision applications, including medical imaging segmentation, which inversely affects image quality and visual perception. Images that exhibit a clear distinction between bright and dark regions, as well as different colors, provide more details about the scene. Such images are essential for various computer vision applications, including medical imaging segmentation [1], [2], [3], oil spill detection [4], [5], surveillance [6], [7], intelligent transportation [8], [9], electrical inspection [10], [11], and imaging visualization [12], [13], [14]. Several low-light image enhancement techniques have emerged, encompassing learning-free methods such as histogram-based algorithms, Retinex-based algorithms [15],

The associate editor coordinating the review of this manuscript and approving it for publication was Yongjie Li.

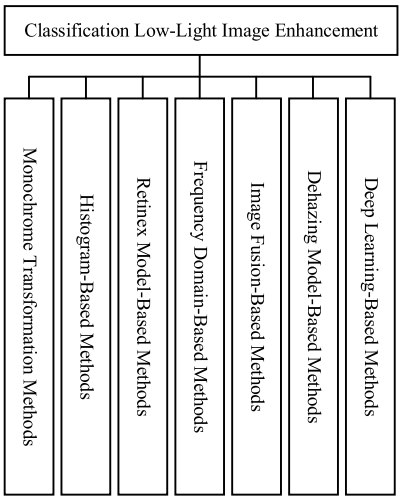

FIGURE 1. Classification of low-light image enhancement procedures.

[16], [17], [18], [19], and learning-based methods like neural network-based algorithms [20], [21], [22], as depicted in Fig. 1.

Among the notable trailer-based low-light image enhancement algorithms, the Fusion-based method for weakly illuminated images (MF) [23] stands out. Inspired by the Retinex theory, MF decomposes images into reflectance and illumination components, enhances them using the sigmoid function and adaptive Histogram Equalization (HE), and fuses them with adaptive weights in a multiscale manner. However, the resulting enhanced image often compromises between visualized details, local contrast improvement, and the preservation of the natural feel of the image.

Another method for low-light image enhancement is LIME (Low-light Image Enhancement via Illumination Map Estimation), which estimates the illumination map for each pixel and adjusts pixel brightness accordingly. However, LIME has drawbacks, such as introducing noise or artifacts, especially in dark regions [24], and over-enhancing pixels, leading to overly bright images with reduced details and contrast. Variants like LIME-Net, LIME-D, and LIME-GAN leverage deep neural networks, denoising techniques, and generative adversarial networks to refine the illumination map and enhance the resulting image quality [25].

Learning-based methods have significantly empowered researchers to tackle challenges associated with inadequately illuminated images in low-light enhancement. The Robust Low-Light Enhancement via Low-Rank Regularized Retinex Model (LR3M) [26] estimates piecewise smoothed illumination and noise-suppressed reflectance but requires improvement in enhancing image details and contrast [27]. Learning Multiscale Photo Exposure Correction (LMSPEC) [21] introduces a coarse-to-fine Deep Neural Network (DNN) model for enhancing color and detail. While it enhances overall contrast and preserves realistic colors, it may yield unsatisfactory results in regions with insufficient semantic information [21].

TABLE 1. Comparison of different low-light algorithms.

Algorithm	Description	Advantages	Drawbacks
MF [23]	Draws from Retinex theory, enhances reflectance and illumination components using sigmoid function and adaptive HE, and multi-scale fusion	Enhance low-light images	Compromises between visualized details and local contrast
LIME [24]	Estimates illumination map for each pixel and adjusts pixel brightness accordingly	Improve image brightness	Introduce noise/artifacts, over-enhancement
Variants of LIME [25] (LIME-Net), LIME-D), LIME-GAN)	Use deep CNNs and denoising techniques to improve illumination map	Enhance image quality	Require extensive training data
LR3M [26]	Estimate piecewise smoothed illumination and noise-suppressed reflectance	Reduce noise	Falls short in enhancing image details and contrast
LMSPEC [21]	Coarse-to-fine DNN model for color and detail enhancement	Enhances contrast and preserves colors	Produces unsatisfactory result in regions with insufficient information
SCI [22]	Features self-calibrated module, achieves exposure stability, reduces complexity	Stable exposure	Require extensive training data, challenges in computational complexity

Despite promising findings, this technology requires further maturity, as algorithms frequently excel in specific aspects.

The Self-Calibrated Illumination (SCI) learning-based framework [22] features a self-calibrated module for illumination learning, achieving exposure stability and reduced computational complexity. However, this approach necessitates extensive training datasets and faces challenges in balancing speed and performance trade-offs [22]. These advancements illustrate the ongoing efforts to enhance low-light image quality, each with its strengths and limitations, signaling the need for continuous refinement and exploration in this domain. A detailed summary of these challenges is provided in TABLE 1.

This paper presents a novel approach to enhance low-quality images by leveraging an improved Retinex theory and a color correction algorithm. The primary objective is to restore the natural appearance and colors of the images while avoiding the introduction of artifacts or noise. The key contributions of this work include:

• Innovative Reflectance Estimation: The introduction of a novel strategy for estimating the reflectance component based on an adaptive Retinex model. This preserves image details and contrasts effectively.

• New Adaptive Gamma Correction: The development of an adaptive gamma correction algorithm that dynamically adjusts brightness and saturation based on luminance distribution, thereby reducing color distortion, and enhancing overall visual quality.

• Logarithm Domain Fractional Stretching Approach: This step enhances the image's overall appearance and realism, normalizes brightness, and balances color saturation.

• State-of-The-Art Techniques Comparison Results and Validation: A comprehensive demonstration of the effectiveness and superiority of the proposed method over other state-of-the-art techniques, validated on various public datasets. The results showcase the method's ability to improve image contrast and maintain color fidelity.

Combining these contributions offers a holistic solution for enhancing low-quality images, ensuring a more faithful representation of the natural scene. The empirical validation further establishes its competitive edge over existing methods, positioning it as a valuable advancement in image enhancement. The rest of the paper is summarized as follows: Section II provides a brief overview of the Retinex theory in image processing. Section III presents the details of the proposed framework. Subjective and objective comparisons are reported in Section IV. We conclude our research in Section V.

II. RELATED WORKS

Recently, various low-light enhancement algorithms have been developed. They can be categorized into three groups: histogram equalization (HE)-based, deep learning-based, and Retinex-based. HE-based methods adjust the properties of an image to expand its dynamic range, effectively brightening dark images. However, these methods often require assistance to adequately adjust the detailed information in the image. Learning-based approaches rely on deep neural networks. However, their effectiveness heavily relies on large amounts of high-quality labeled data, making them labor-intensive and time-consuming. Determining the ground truth and acquiring ideal pairs of low-light and normal-light images is also challenging to accurately isolate the specific degradation caused by low-light conditions. The Retinex theory, proposed by Land et al. [28], offers a robust and flexible framework for low-light image enhancement. It decomposes an image into illumination and reflectance components, providing a basis for various Retinex-based algorithms.

A. SINGLE-SCALE RETINEX (SSR)

Retinex constitutes a prominent conceptual framework on color constancy, introduced by Land and McCann [28]. Human vision perceives relative brightness instead of absolute brightness, and the human visual system is insensitive to gradually changing illumination [16].

Retinex theory is a computational model for human color vision, elucidating how the visual system perceives colors and lightness consistently across various lighting conditions – an occurrence recognized as color constancy. Moreover, the theory accommodates the Land effect, which denotes the observation that certain colors become discernible only when two or more different light sources illuminate a scene.

According to Retinex theory, the human visual system consists of three independent channels, called Retinexes, that process the information from the long-wave, medium-wave, and short-wave sensitive cones in the retina. Each retinex computes the ratio of light reflected from each point in the scene to the average of the light reflected from its surrounding area. This ratio is then used to determine the lightness value for each point in each channel. The triplet of lightness values from the three channels corresponds to the perceived color and reflectance of each point in the scene.

Retinex theory assumes that the illumination in a scene varies smoothly and that there are no sharp edges or abrupt changes in brightness. This assumption enables the Retinex algorithm to distinguish between illumination and reflectance by analyzing both local and global information. The theory also predicts that color sensations are influenced not only by the local receptor responses but also by the content and context of the entire image.

Retinex theory has undergone testing and received support from various experiments and applications. For instance, Land demonstrated the ability to generate different colors by employing various combinations of colored lights to illuminate a black-and-white image. Additionally, he illustrated that altering the color of the surrounding environment could influence the perceived color of an object. Furthermore, Retinex theory has served as a source of inspiration for numerous computational models and algorithms. These models aim to emulate human color vision and undertake tasks such as low-light image enhancement and color correction.

The Retinex model explains that the observed image, $\boldsymbol{I}$, consists of a reflectance component, $\boldsymbol{\mathcal{R}}$, and a luminance component, $\boldsymbol{\mathcal{L}}$. The model can be represented as follows:

$$\boldsymbol{I} = \boldsymbol{\mathcal{R}} \,.\, \boldsymbol{\mathcal{L}} \tag{1}$$

Computer simulations have demonstrated that SSR methods exhibit sensitivity to high-frequency components, enabling effective enhancement of edge information in an image. However, one drawback is that the resulting enhanced image often appears unnatural and can be over-enhanced, compromising its visual quality. Additionally, the edges are not sharp enough, and high-frequency details cannot be significantly improved. Meanwhile, Retinex poses a mathematically ill-posed problem; consequently, several decomposition approaches have been proposed.

B. MULTI-SCALE RETINEX (MSR)

Jobson et al. [21] applied the traditional Retinex-based model, specifically the SSR technique, to improve images. Subsequently, they expended SSR and formulated the Multiscale Retinex (MSR) technique, which integrates multiple filtering kernels. Each scale represents varying levels of spatial content, ranging from global illumination variations to local details and textures. So, the reflectance component can be

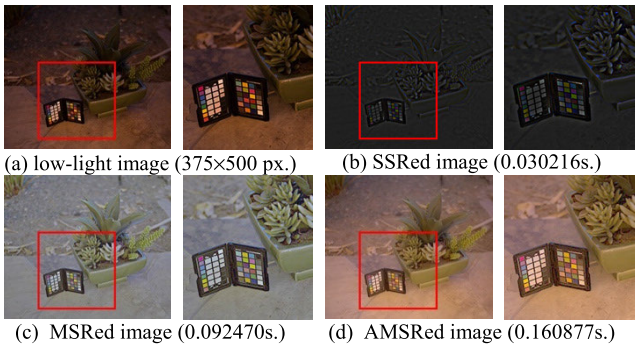

(a) low-light image (375×500 px.) (b) SSRed image (0.030216s.)
(c) MSRed image (0.092470s.) (d) AMSRed image (0.160877s.)

FIGURE 2. Example of different retinex models.

described as:

$$\log(\mathcal{R}) = \sum_{k=1}^{N} \omega_k \cdot (\log(I) - \log(I \otimes F_k(\sigma_k))) \quad (2)$$

where ω_k denotes the weight associated with the k^{th} scale, $F_k(\sigma_k)$ represents a Gaussian filter, σ_k is a standard deviation of the filter, I is a given image, and N refers to the total number of scales.

C. ADAPTIVE MULTI-SCALE RETINEX (AMSR)

Conventional image enhancement methods often encounter challenges in generating satisfactory, distortion-free images when dealing with images containing both overexposed and underexposed areas. The traditional Multiscale Retinex (MSR) approach proves inadequate in effectively addressing this issue, relying on a weighted sum of several Single-Scale Retinex (SSR) outputs for local image contrast enhancement and dynamic range compression [29]. In contrast, the AMSR approach provides a solution by introducing adaptive weights computed based on the content of the input image. The adaptive weight can be calculated as:

$$\omega_k = \frac{p_k}{\sum_{k=1}^{N} p_k}; \quad p_k = e^{-\frac{1}{\sqrt{2}}\left(\frac{X_k - \mu_k}{\sigma_k}\right)^2} \quad (3)$$

where p_k is a likelihood probability function, X_k denotes an input luminance image with the k^{th} scale. μ_k represents the mean value of the image, σ_k refers to the standard deviation of the image, and N refers to the total number of scales.

D. CHALLENGES

The Retinex theory, initially proposed by Land et al., is a widely recognized framework in image processing that enhances the visibility and quality of images, particularly in low-light environmental conditions. It is considered one of the most promising approaches to image enhancement. However, despite its effectiveness in many cases, the application of the Retinex theory faces various challenges, particularly in the context of low-light image enhancement. These challenges include the potential for color shifts and the occurrence of artifacts, which may vary across different versions of the Retinex theory. A detailed summary of these challenges is provided in TABLE 2, and illustrative examples are presented in Fig. 2.

TABLE 2. Comparison of different retinex algorithms.

	Single-Scale Retinex (SSR) [28]	Multi-Scale Retinex (MSR) [17]	Adaptive Multiscale Retinex (AMSR) [29]
Methodology	Applies a single-scale filter	Utilizes multiple-scale filters	Uses adaptive multiple-scale filters
Enhancement Level	Global Enhancement	Global and local enhancement	Global and local enhancement
Image Dynamics	Lead to over/under-enhancement	Reduces over/under-enhancement artifacts	Reduces over/under-enhancement artifacts
Complexity	Low	Moderate	High
Details	Loss of fine details	Preserves fine details	Preserves fine details
Colors	Loss of colors	Illustrates artificial colors	Preserves realistic colors
Applications	Basic image enhancement	Generate image enhancement	Challenging lighting conditions

The SSR algorithm is a straightforward method that offers reduced processing time. However, its effectiveness is compromised by its inability to visualize local details, as it operates on a fixed scale. Additionally, SSR may not adequately address local contrast enhancement, potentially resulting in the loss of fine details, as depicted in Fig. 2(b).

The MSR algorithm represents an extension of SSR, operating on multiple levels to enhance low-light images. Nevertheless, adopting multiple scales introduces increased computational complexity and processing resource requirements. The MSR imposes a trade-off between improving global contrast and preserving important details. In certain cases, this trade-off may lead to the loss of crucial chromatic information, as illustrated in Fig. 2(c).

The AMSR algorithm constitutes an advanced version of the Retinex theory, aiming to overcome some of the limitations of previous approaches by dynamically adapting to image characteristics at multiple scales. However, AMSR has its own limitations, the most prominent being its high computational complexity compared to SSR and MSR algorithms. Nonetheless, visual analysis demonstrates that AMSR plays an essential role in preserving global and local contrast, enhancing important details while preserving overall brightness and realistic color, as shown in Fig. 2(d).

III. NEW STRATEGY FOR ESTIMATING THE REFLECTANCE COMPONENT OF THE IMAGE BASED ON AN ADAPTIVE RETINEX MODEL

A. PROPOSED AMSR

The Retinex model can be expressed in a variety of mathematical forms. Let's consider a new Retinex model, $\boldsymbol{I}$ =

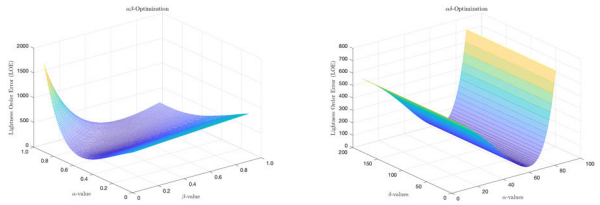

(a) Parameters optimization for the case 1 (b) Parameters optimization for the case 2

FIGURE 3. Constants optimized by minimizing lightness order error (LOE) values.

$f(\mathcal{R}, \mathcal{L})$, where $f(\mathcal{R}, \mathcal{L})$ is a function, for example:

$$f(\mathcal{R}, \mathcal{L}) = \tau \mathcal{R}^{\lambda} \cdot \mathcal{L}^{\vartheta} \tag{4}$$

where τ, λ and γ are an arbitrary constant, $\mathcal{R}$ denotes a reflectance component, and $\mathcal{L}$ refers to a luminance component. If $\tau = \lambda = \vartheta = 1$, then we get the classical Retinex model.

The problem is first converted to the logarithmic domain, where $\boldsymbol{I} = \log(I + \varepsilon)$, $\mathcal{L} = \log(\mathcal{L} + \varepsilon)$, and $\mathcal{R} = \log(\mathcal{R} + \varepsilon)$. This step is motivated by both mathematical and physiological considerations, as additions are typically easier to compute than multiplications. If a high-quality intrinsic image decomposition is available, it can be used to manipulate the layer-remapping operators in various illumination-related tasks.

Let's investigate the different cases. Case 1: $\tau = 1$, λ and ϑ are an arbitrary constant.

$$f(\mathcal{R}, \mathcal{L}) = \mathcal{R}^{\lambda} \cdot \mathcal{L}^{\vartheta} \tag{5}$$

$$\log(I + \varepsilon) = \lambda \log(\mathcal{R} + \varepsilon) + \vartheta \log(\mathcal{L} + \varepsilon) \tag{6}$$

$$\lambda \log(\mathcal{R} + \varepsilon) = \log(I + \varepsilon) - \vartheta \log(\mathcal{L} + \varepsilon) \tag{7}$$

$$\log(\mathcal{R} + \varepsilon) = \alpha \log(I + \varepsilon) - \beta \log(I \otimes F_k(\sigma_k) + \varepsilon) \tag{8}$$

Case 2: τ, λ and γ are an arbitrary constant.

$$f(\mathcal{R}, \mathcal{L}) = \tau \mathcal{R}^{\lambda} \cdot \mathcal{L}^{\vartheta} \tag{9}$$

$$\log(I + \varepsilon) = \log(\tau + \varepsilon) + \lambda \log(\mathcal{R} + \varepsilon) + \vartheta \log(\mathcal{L} + \varepsilon) \tag{10}$$

$$\lambda \log(\mathcal{R} + \varepsilon) = \log(I + \varepsilon) - \vartheta \log(\mathcal{L} + \varepsilon) - \log(\tau + \varepsilon) \tag{11}$$

$$\log(\mathcal{R} + \varepsilon) = \alpha \log(I + \varepsilon) + \beta \log(\mathcal{L} + \varepsilon) + \delta \tag{12}$$

$$\log(\mathcal{R} + \varepsilon) = \alpha \log(I + \varepsilon) + \beta \log(I \otimes F_k(\sigma_k) + \varepsilon) + \delta \tag{13}$$

where α denotes the brightness parameter, β represents the edge enhancement parameter, and δ is a constant. $F_k(\sigma_k)$ represents a Gaussian filter with the k^{th} scale, σ_k is a standard deviation of the filter, I is a given image, ε is an offset value, and N refers to the total number of scales. The determination of these parameters is conducted using the Lightness Order Error (LOE) measure [30], employing the LOL dataset, as depicted in Fig. 3.

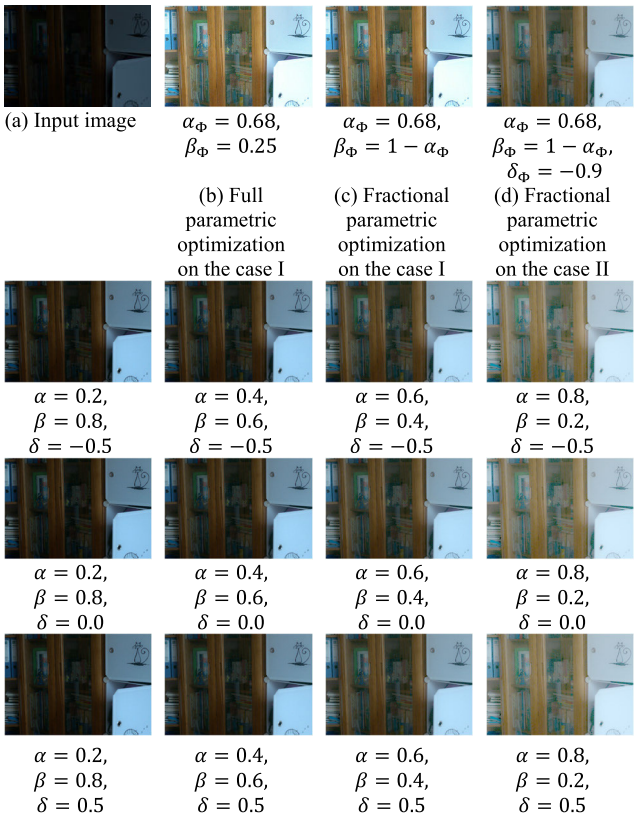

FIGURE 4. Illumination and reflectance mapping in the logarithmic domain.

The optimal α and β can be described as:

$$\alpha_\Phi = \underset{\alpha}{\operatorname{argmin}}\left(LOE(I, R)\right) \tag{14}$$

$$\beta_\Phi = \underset{\alpha}{\operatorname{argmin}}\left(LOE\left(I_{ref}, R\right)\right) \tag{15}$$

where $LOE(\cdot)$ denotes a lightness order error function, α denotes the brightness parameter, I_{ref} refers to a reference image, and R represent a Retinex decomposition image.

The modified Retinex can be applied to the AMSR model. The modified AMSR model can be described as:

$$\log(\mathcal{R} + \varepsilon) = \sum_{k=1}^{N} \omega_k \cdot \begin{pmatrix} \lambda \log(\mathcal{R} + \varepsilon) \\ -\vartheta \log(I \otimes F_k(\sigma_k) + \varepsilon) \end{pmatrix} + \log(\tau + \varepsilon) \tag{16}$$

where ω_k is a weight, $\mathcal{R}$ represents a reflectance component, I is a given image, and N refers to the total number of the filter scales. $F_k(\sigma_k)$ represents a Gaussian filter with the k^{th} scale, ε is an offset value, τ, λ and γ are an arbitrary constant, and σ_k denotes the width of a Gaussian filter associated with the following expression.

$$\sigma_k(m, n, s) = \frac{\min\{m, n\}}{10s} \tag{17}$$

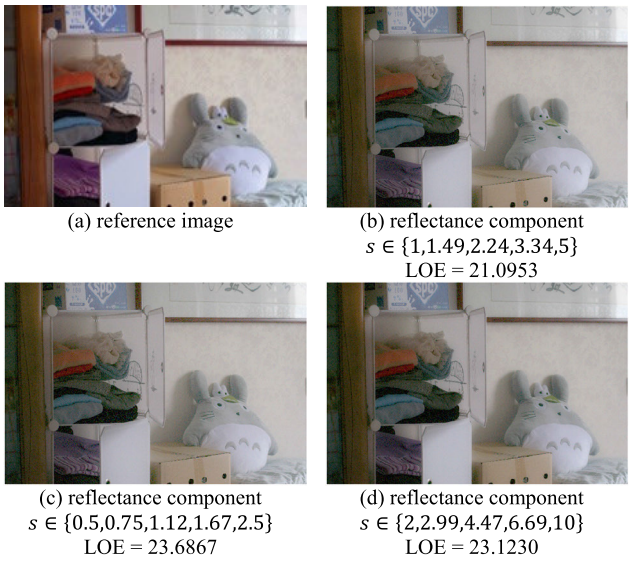

FIGURE 5. Comparison among different sets of *s*.

FIGURE 6. Comparison OFAMSR methods.

where m and n refers to the size of an image, and s is a parametric set. Similar to the MSR algorithm, $\sigma_k\ (m, n, s)$ determines the smoothness of the low-frequency components of the image. A large sigma results in a smoother filtered image, whereas a smaller sigma preserves more fine details, but amplifies noises as shown in Fig. 4.

The set $\{s\}$ represents a parametric set that depends on the image size. Its computation is conducted within a logarithmic scale encompassing the range from 10^1 and 10^k where k refers to the number of Retinex scale. In this paper, s is explicitly defined as $\{1, 1.49, 2.24, 3.34, 5\}$, based on the demonstrated the less LOE value as illustrated in Fig. 5. To visualize the reflection image component of the Retinex decomposition, it can be calculated as:

$$R = \frac{e^{\log(\mathcal{R}-\varepsilon)} - \min\left\{e^{\log(\mathcal{R}-\varepsilon)}\right\}}{\max\left\{e^{\log(\mathcal{R}-\varepsilon)}\right\} - \min\left\{e^{\log(\mathcal{R}-\varepsilon)}\right\}} \tag{18}$$

where $\mathcal{R}$ represents a reflection image component, and ε denotes an offset value.

In Fig. 6, a comparison is presented between the existing AMSR method as described in [29] and the proposed AMSR method. The conventional approach effectively introduces notable details under low-light and backlit conditions. This technique employs a composite of different linear stretching functions within the framework of the MSR decomposition. However, the resulting image exhibits certain unsatisfactory artifacts, such as over-brightness, loss of some details, and color saturation. Conversely, the proposed AMSR method adeptly preserves significant details and accurately retains the original color representation without undesirable artifacts.

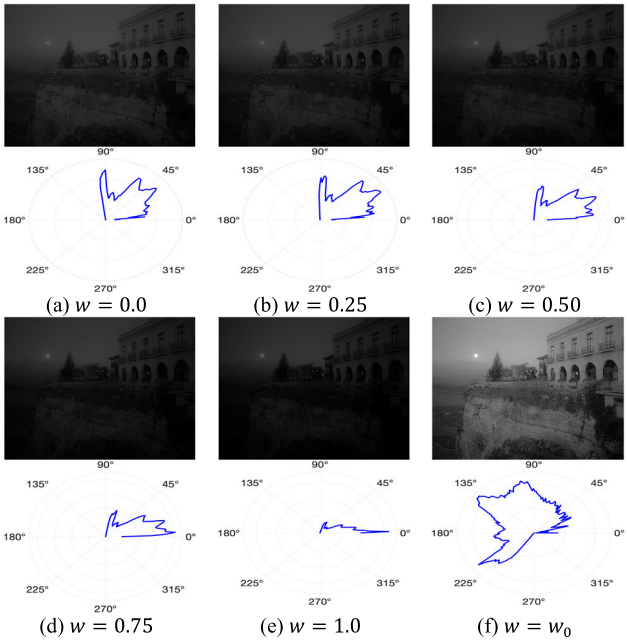

FIGURE 7. Visualized image of the weight effects with different ω.

B. FRACTIONAL STRETCHING

In this section, we introduce Fractional Stretching, which is a technique that addresses the issue of luminance saturation in images. It is a technique that applies a non-linear function to the image's intensity values. This function has the effect of stretching the range of intensity values, which can make the image appear more contrasty. Let $L^*_{i,j}$ denote a luma image component, which consists of intensity levels, on the $L^*a^*b^*$ color-space represented by the set $L^*_{i,j} = \left\{L^*_{min}, L^*_{min+1}, \ldots, L^*_{max}\right\}$. The permitted range between L^*_{min} and L^*_{max} is transformed non-linearly to the range between L'_{min} and L'_{max}. The resulting fractional stretched images, denoted as $\mathcal{S}_{i,j}$, can be calculated by using the following function:

$$F\mathcal{S}_{i,j} = \frac{1}{T}\sum\nolimits_{t=1}^{T}\left(\frac{\left(L^*_{max} - L^*_{min}\right)\left(L^*_{i,j} - L^*_{min}\right)}{L'_{max}. - L'_{min}}\right)^{\psi_t} \tag{19}$$

Here, T represents the total number of fractional stretching functions. The value of ψ_t depends on the following conditions:

$$\psi_t = \begin{cases} 0.1, 0.11, \ldots, 0.5, & \tau \leq \dfrac{x_{L-1}}{2} \\ 0.5, 0.51, \ldots, 1.0, & \tau > \dfrac{x_{L-1}}{2} \end{cases} \tag{20}$$

where τ denotes a global mean of a luma image component, and represents an image-dependent threshold, x_{L-1}

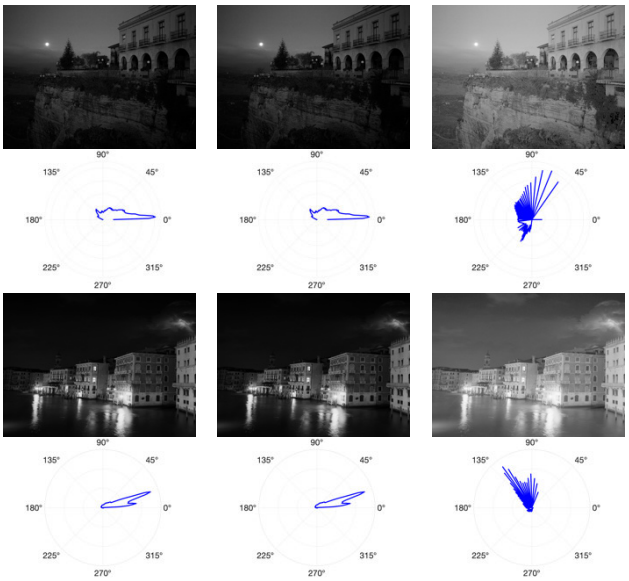

(a) given image (b) linear stretched image (c) fractional stretched image

FIGURE 8. Comparison between fractional stretching and linear stretching.

represents the total number of intensity levels.

$$\mathcal{S}_{i,j} = w \cdot F\mathcal{S}_{i,j} + (1 - w)\, L^*_{i,j} \tag{21}$$

where w refers to a weight, $L^*_{i,j}$ denotes a luma image component. To discuss the understanding of how w controls image brightness, the relationship between w and image brightness can be direct or indirect. w may influence pixel values or other factors contributing to image brightness. By manipulating the value of w, different levels of brightness can be observed in Fig. 7.

For instance, increasing the value of w can improve brightness, resulting in a lighter appearance of the image. Conversely, decreasing w can dim brightness, leading to a darker image. In this paper, an appropriate value for w, denoted as ω_0, can be calculated as:

$$w_0 = \frac{\mathcal{S}_{i,j}}{\max\left\{\mathcal{S}_{i,j}\right\}}; \quad \max\left\{\mathcal{S}_{i,j}\right\} \neq 0 \tag{22}$$

The resulting image of w_0, as illustrated in Fig. 7(f), delivers a wide dynamic range of luminance distribution, thereby increasing overall contrast and avoiding over-brightness artifacts.

Fig. 8 represents a comparison between the classical linear stretching function and the fractional function. The illustrative images used for the comparison consist of both underexposed regions and small overexposed regions. The linear stretching algorithm proves to be ineffective in adequately addressing the low-contrast issue. Conversely, the fractional stretched images exhibit the ability to effectively convey significant information. These images demonstrate improved visualization of details and enhanced contrast compared to the linear stretching algorithm.

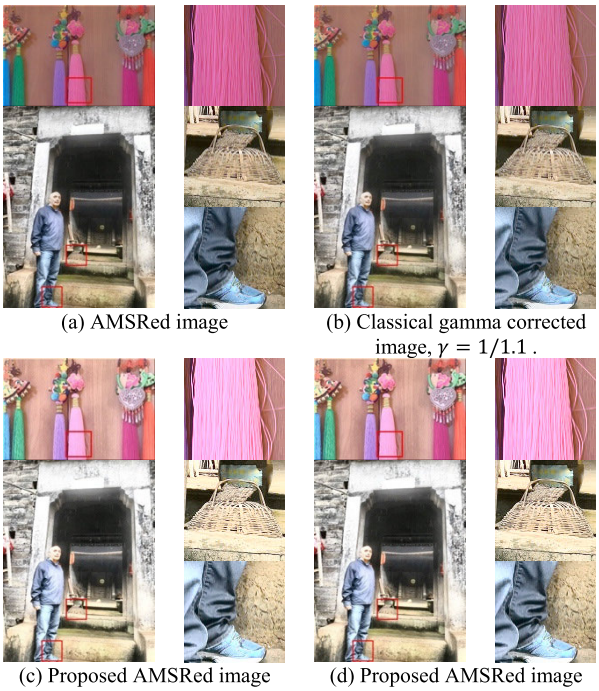

(a) AMSRed image (b) Classical gamma corrected image, $\gamma = 1/1.1$.

(c) Proposed AMSRed image with the adaptive gamma correction [31] (d) Proposed AMSRed image with the proposed gamma correction

FIGURE 9. Comparison among different gamma correction parameters.

C. ADAPTIVE GAMMA CORRECTION

It is a technique that applies a different gamma correction value to each pixel in an image. This is done to adjust the contrast of each pixel based on its local surroundings, improving the perceptual quality of images on various electronic devices. Traditional gamma correction methods employ a fixed gamma parameter, which is not optimal for all image regions, leading to underexposure or overexposure in different regions. To address these limitations, the adaptive gamma correction algorithm based on the combination of image-dependent luminance distribution functions is presented as:

$$f\left(L^*\right) = L^*_{max}\left[\left(\frac{L^*}{L^*_{max}}\right)^{\left(\frac{\ln\left(\frac{c(L^*)}{p(L^*)-1}+2\right)}{\ln(2)}\right)}\right] \tag{23}$$

where L^* denotes the luma component on the *Lab* colorspace, L^*_{max} refers to the maximum of the luma component, $c\left(L^*\right)$ represents an image-dependent cumulative distribution function, and $p\left(L^*\right)$ is an image-dependent probability.

The analysis of Fig. 9 reveals evidence that the classical gamma correction method leads to underexposed details and sub-optimal visual appearance. This result illustrates the limitations of using a fixed gamma value for all pixels in the image. It fails to adapt to local luminance variations. In contrast, the adaptive gamma correction approach in [31] demonstrates an attempt to address this limitation by adjusting gamma values. However, it introduces an over-brightness

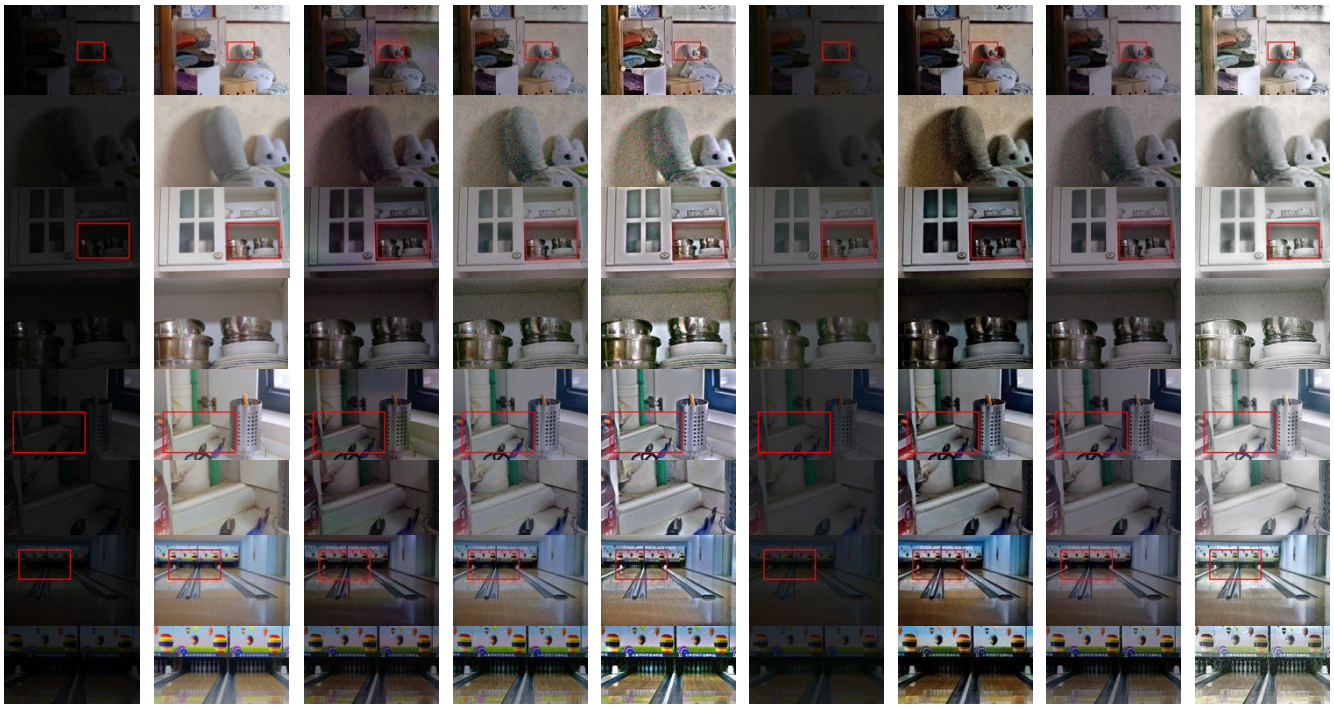

(a) given image | (b) Ground truth | (c) CLAHE [32] | (d) MF [23] | (e) LIME [24] | (f) LR3M [26] | (g)LMSPEC [21] | (h) SCI [22] | (i) Proposed

FIGURE 10. Comparisons of traditional low-light image enhancement methods on the LOL dataset [33].

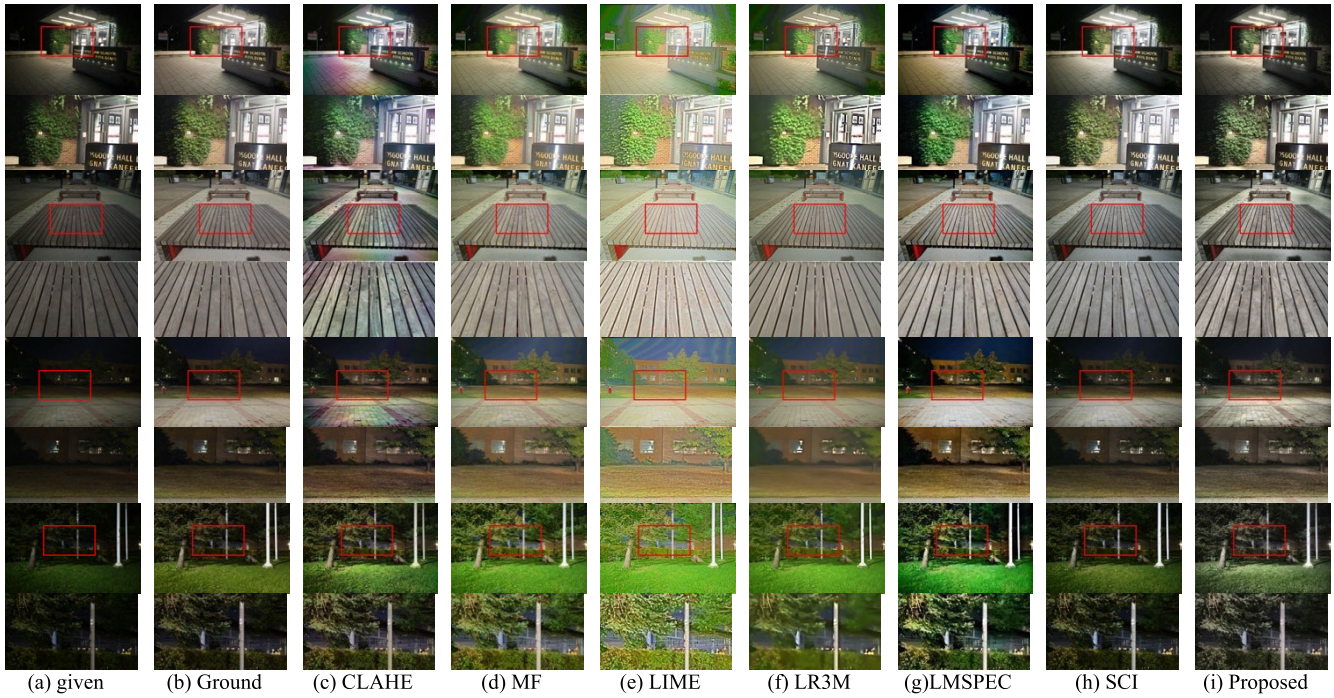

(a) given image | (b) Ground truth | (c) CLAHE [32] | (d) MF [23] | (e) LIME [24] | (f) LR3M [26] | (g)LMSPEC [21] | (h) SCI [22] | (i) Proposed

FIGURE 11. Comparisons of traditional low-light image enhancement methods on the ISP dataset [34].

artifact, resulting in losing image details. The proposed gamma correction method shows some challenges in overcoming these challenges. It presents a potential improvement over classical and state-of-the-art adaptive techniques by preserving image details and effectively reducing the issue associated with over-brightness.

TABLE 3. Comparison of image quality assessments (IQAs).

Type of IQA	Advantages	Disadvantages	Examples
FR-IQA [35]	Most accurate, commonly used, and suitable for precise comparisons.	Requires a reference image, and less suitable for real-time analysis.	• Mean Squared Error (MSE) • Peak Single-to-Noise Ratio (PSNR) • Structural Similarity Index (SSIM) • Multiscale Structural Similarity Index (MS-SSIM) • Lightness Order Error (LOE)
NR-IQA [36]	Least restrictive, and suitable for real-time analysis	Least accurate and not be suitable for high precision comparisons.	• Enhancement Measure (EME) • Blind/Referenceless Image Spatial quality Evaluator (BRISQUE) • Natural Image Quality Evaluator (NIQE) • Image Quality Assessment based on Local Gradient Features (LGF-IQA)

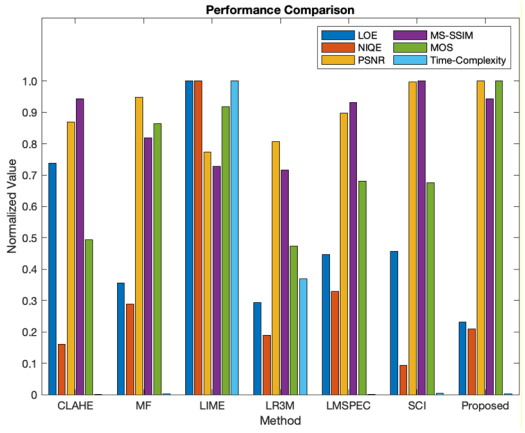

FIGURE 12. Performace comparison.

IV. EXPERIMENTAL RESULT ANALYSIS

In this section, we first analyze the proposed and state-of-the-art methods using quantitative and qualitative assessments. The comparative methods used are CLAHE [32], MF [23], LIME [24], LR3M [26], LMSPEC [21], and SCI [22]. All comparative computer simulation experiments were performed in MATLAB R2022b on a PC running MacOS with an Intel®Core™ i9 CPU @ 2.3GHz and 16 GB of memory. All test images and reference images come from the publicly available LOL [33] and ISP [34] datasets. Finally, we performed the proposed method on images generated in severe low-light environments to verify its effectiveness.

A. SUBJECTIVE EVALUATION

The computer simulation results are depicted Fig. 10. Fig. 10(a) shows the low-light images and their extracted regions. Fig. 10(b-i) presents the resulting images of various methods, including CLAHE [32], MF [23], LIME [24], LR3M [26], LMSPEC [21], and SCI [22], and the proposed method. The extracted images corresponding to the rectangular box in Fig. 10 are shown in the next row.

According to the observations in the figure, images generated by various enhancement techniques exhibit varying levels of visual quality when compared to the original image.

Comparing the proposed method with the conventional image enhancement technique: the image generated by the linear mapping function, CLAHE [32], exhibits poor visual quality. The degree of scene visualization is insufficient to deliver important information effectively. In contrast, the proposed method has improved the clarity and contrast of the enhanced images, resulting in an enhancement effect.

Comparing the proposed method with the state-of-the-art image enhancement techniques: the MF [27] and the LIME [28] have demonstrated their ability to enhance image intensity effectively. However, the MF method produces under-exposed regions with noise, while the LIME method produces a noticeable noise effect throughout the image. The LR3M method [26] yields only a modest degree of enhancement and falls short of enhancing significant details. Specifically, the method is limited to restoring details in severely dark regions. Compared to other methods such as the LMSPEC method [21] and the SCI method [22], our proposed method and the aforementioned methods maintain a balance among color, contrast, brightness, and other visual attributes. However, compared to our proposed method, the LMSPEC method falls short in providing uniform results for extremely dark regions in terms of overall image quality. Furthermore, upon comparing the local content information in the extracted regions, artifacts such as noise and blur caused by insufficient enhancement are apparent in both the LMSPEC and SCI methods. Additionally, the LMSPEC method displays strong shadows in local areas. On the other hand, our proposed method can emphasize significant information without over-enhancement and noise amplification throughout the entire image. It can also generate a better sense of clarity and color in scenes.

B. OBJECTIVE EVALUATION

Due to the different features of various low-light image enhancement methods, subjective assessment becomes an inevitable evaluation approach. Consequently, the computational assessment of image quality is considered an alternative method. The evaluation of image quality is a common practice for measuring the efficacy of diverse methods. The image quality assessment (IQA) can be classified

(a) Ground truth (b) MF [23] (c) LIME [24] (d) LR3M [26] (e) Proposed

FIGURE 13. Comparisons of traditional low-light image enhancement with its reference image.

into two categories: Full-Reference IQA (FR-IQA) [35], and No-Reference IQA (NR-IQA) [36].

FR-IQAs require a reference image for comparison, while NR-IQAs do not. In this paper, several FR-IQA metrics, namely the multiscale structural similarity (MS-SSIM) [39], the lightness order error (LOE) [30], and the peak single-to-noise ratio (PSNR) [38], MOS [40], were employed to evaluate the performance of various low-light image enhancement methods. Higher MS-SSIM and PSNR scores indicate richer detail visualization, while a lower LOE value signifies better quality. For NR-IQA, the Natural Image Quality Evaluator (NIQE) [37] was used to assess the efficacy of low-light enhanced images. A lower NIQE score corresponds to superior performance. TABLE 4 and Fig. 12 illustrate the objective evaluation results of state-of-the-art methods.

In terms of FR-IQA metrics, the proposed method achieved superior results for LOE [30], PSNR [38], and MOS [40], demonstrating its effectiveness in enhancing image quality. While the proposed method exhibits a slightly higher computational complexity compared to the MF method, the resulting improvement in image quality justifies the increased processing time. Also, the proposed method can preserve structural details by more than 83% compared to the ground truth. For the NIQE metric, the proposed method attempts to preserve more details in the enhanced image. Occasionally, the proposed enhancement affects the visual quality of natural images, such as loss of details.

The visual comparison depicted in Fig. 13 provides a deeper insight into the advantages of the proposed method. Compared to the reference images, the proposed images exhibit a noticeable improvement in preserving and depicting finer details. However, a slight decline in the MS-SSIM metric is observed. The proposed method's emphasis on enhancing structural details leads to a marginal reduction in MS-SSIM. This is because the balance between structural image preservation and contrast enhancement is intricately related.

TABLE 4. Results of image quality measure metrics with different methods and average time-complexity per an image.

Method / Processing Time	LOE [30] ↓	NIQE [37] ↓	PSNR [38] ↑	MS-SSIM [39] ↑	MOS [40] ↑
CLAHE [32] / 0.0152 sec.	592.70	392.56	15.66	0.83	2.03
MF [23] / 0.2153 sec.	285.63	709.89	17.09	0.72	3.55
LIME [24] / 118.3293 sec.	803.96	2,454.53	13.93	0.64	3.77
LR3M [26] / 43.7140 sec.	236.79	465.41	14.54	0.63	1.95
LMSPEC [21] / 0.1108 sec.	358.86	809.65	16.18	0.82	2.80
SCI [22] / 0.5967 sec.	367.21	**229.37**	17.97	**0.88**	2.78
Proposed / 0.3951 sec.	**185.43**	512.39	**18.02**	0.83	**4.11**

V. CONCLUSION

In this study, we have addressed the challenge of non-uniform illumination in low-light conditions by employing Retinex decomposition and color image enhancement techniques. Our approach involves transforming the Retinex-based imaging components into the *Lab* color-space and applying fractional stretching algorithms to individually enhance the illuminance

and reflectance components. By adaptively adjusting the weight parameters of the illuminance distribution, we fuse the enhanced imaging components to normalize brightness and information.

Furthermore, we improve the contrast of the color image by performing local image enhancement on an extended grayscale plane. This approach significantly enhances the image's visual quality, effectively preserving both contrast and brightness. Comparative evaluations against state-of-the-art supervised and unsupervised methods demonstrate that our framework achieves visually pleasing intrinsic components and outperforms unsupervised competitors regarding subjective observations and objective image quality assessments. The proposed method exhibits adaptability in enhancing images with non-uniform illumination, resulting in natural-looking outputs.

Its potential applications span various fields, including low-light video enhancement, nighttime surveillance, and scene restoration. However, it is essential to note that the denoising process currently contributes significantly to the overall time complexity. Future research efforts will focus on reducing and improving the denoising process's efficiency to enhance the method's overall performance. Nevertheless, the decomposition of the proposed Retinex model comprises a significant portion of the computational complexity associated with the overall process. Consequently, the optimization and selection of efficient arbitrary constants will be a crucial area of research in the future.

REFERENCES

[1] A. Oulefki, S. Agaian, T. Trongtirakul, S. Benbelkacem, D. Aouam, N. Zenati-Henda, and M.-L. Abdelli, "Virtual reality visualization for computerized COVID-19 lesion segmentation and interpretation," *Biomed. Signal Process. Control*, vol. 73, Mar. 2022, Art. no. 103371, doi: 10.1016/j.bspc.2021.103371.

[2] S. Benbelkacem, A. Oulefki, S. Agaian, N. Zenati-Henda, T. Trongtirakul, D. Aouam, M. Masmoudi, and M. Zemmouri, "COVI3D: Automatic COVID-19 CT image-based classification and visualization platform utilizing virtual and augmented reality technologies," *Diagnostics*, vol. 12, no. 3, p. 649, Mar. 2022, doi: 10.3390/diagnostics12030649.

[3] A. Oulefki, S. Agaian, T. Trongtirakul, and A. Kassah Laouar, "Automatic COVID-19 lung infected region segmentation and measurement using CT-scans images," *Pattern Recognit.*, vol. 114, Jun. 2021, Art. no. 107747, doi: 10.1016/j.patcog.2020.107747.

[4] T. Trongtirakul, S. Agaian, A. Oulefki, and K. Panetta, "Method for remote sensing oil spill applications over thermal and polarimetric imagery," *IEEE J. Ocean. Eng.*, vol. 48, no. 3, pp. 973–987, Jul. 2023, doi: 10.1109/JOE.2023.3245759.

[5] A. Oulefki, T. Trongtirakul, S. Agaian, and W. Chiracharit, "Detection and visualization of oil spill using thermal images," *Proc. SPIE*, vol. 11399, Apr. 2020, Art. no. 113990L.

[6] B. H. Kim, C. Bohak, K. H. Kwon, and M. Y. Kim, "Cross fusion-based low dynamic and saturated image enhancement for infrared search and tracking systems," *IEEE Access*, vol. 8, pp. 15347–15359, 2020, doi: 10.1109/ACCESS.2020.2966794.

[7] M. A. B. Abbass and H.-S. Kang, "Violence detection enhancement by involving convolutional block attention modules into various deep learning architectures: Comprehensive case study for UBI-fights dataset," *IEEE Access*, vol. 11, pp. 37096–37107, 2023, doi: 10.1109/ACCESS.2023.3267409.

[8] Y. Cui and D. Lei, "Optimizing Internet of Things-based intelligent transportation system's information acquisition using deep learning," *IEEE Access*, vol. 11, pp. 11804–11810, 2023, doi: 10.1109/ACCESS.2023.3242116.

[9] X. Guo and X. Guo, "A research on blockchain technology: Urban intelligent transportation systems in developing countries," *IEEE Access*, vol. 11, pp. 40724–40740, 2023, doi: 10.1109/ACCESS.2023.3270100.

[10] T. Trongtirakul and S. Agaian, "Unsupervised and optimized thermal image quality enhancement and visual surveillance applications," *Signal Process., Image Commun.*, vol. 105, Jul. 2022, Art. no. 116714, doi: 10.1016/j.image.2022.116714.

[11] S. Parakul, "Determination of motor efficiency in air condensing unit using thermal image analytics in case the degradation of capacitance," *J. Energy Environ. Technol. Graduate School SIAM Technol. College*, vol. 9, no. 2, pp. 50–61, 2022.

[12] T. Trongtirakul, W. Chiracharit, and S. S. Agaian, "Single backlit image enhancement," *IEEE Access*, vol. 8, pp. 71940–71950, 2020, doi: 10.1109/ACCESS.2020.2987256.

[13] T. Trongtirakul and S. Agaian, "Transmission map optimization for single image dehazing," *Proc. SPIE*, vol. 12100, May 2022, Art. no. 121000C, doi: 10.1117/12.2621831.

[14] T. Trongtirakul and S. Agaian, "Adaptive inertia weight particle swarm algorithm for optimized hyperspectral image enhancement," *Proc. SPIE*, vol. 11734, Apr. 2021, Art. no. 1173403, doi: 10.1117/12.2585548.

[15] J. McCann, "Retinex theory," in *Encyclopedia of Color Science and Technology*, M. R. Luo, Ed. New York, NY, USA: Springer, 2016, pp. 1118–1125.

[16] S. Oishi and N. Fukushima, "Retinex-based relighting for night photography," *Appl. Sci.*, vol. 13, no. 3, p. 1719, Jan. 2023.

[17] D. J. Jobson, Z. Rahman, and G. A. Woodell, "Properties and performance of a center/surround Retinex," *IEEE Trans. Image Process.*, vol. 6, no. 3, pp. 451–462, Mar. 1997, doi: 10.1109/83.557356.

[18] D. Zhang, Y. Huang, X. Xie, and X. Guo, "A variational Retinex model with structure-awareness regularization for single-image low-light enhancement," *IEEE Access*, vol. 11, pp. 50918–50928, 2023, doi: 10.1109/ACCESS.2023.3278734.

[19] H. A. Gasparyan, S. A. Hovhannisyan, S. V. Babayan, and S. S. Agaian, "Iterative Retinex-based decomposition framework for low light visibility restoration," *IEEE Access*, vol. 11, pp. 40298–40313, 2023, doi: 10.1109/ACCESS.2023.3269719.

[20] K. G. Lore, A. Akintayo, and S. Sarkar, "LLNet: A deep autoencoder approach to natural low-light image enhancement," *Pattern Recognit.*, vol. 61, pp. 650–662, Jan. 2017, doi: 10.1016/j.patcog.2016.06.008.

[21] M. Afifi, K. G. Derpanis, B. Ommer, and M. S. Brown, "Learning multi-scale photo exposure correction," in *Proc. IEEE/CVF Conf. Comput. Vis. Pattern Recognit. (CVPR)*, Jun. 2021, pp. 9153–9163, doi: 10.1109/CVPR46437.2021.00904.

[22] L. Ma, T. Ma, R. Liu, X. Fan, and Z. Luo, "Toward fast, flexible, and robust low-light image enhancement," in *Proc. IEEE/CVF Conf. Comput. Vis. Pattern Recognit. (CVPR)*, Jun. 2022, pp. 5627–5636, doi: 10.1109/CVPR52688.2022.00555.

[23] X. Fu, D. Zeng, Y. Huang, Y. Liao, X. Ding, and J. Paisley, "A fusion-based enhancing method for weakly illuminated images," *Signal Process.*, vol. 129, pp. 82–96, Dec. 2016, doi: 10.1016/j.sigpro.2016.05.031.

[24] X. Guo, Y. Li, and H. Ling, "LIME: Low-light image enhancement via illumination map estimation," *IEEE Trans. Image Process.*, vol. 26, no. 2, pp. 982–993, Feb. 2017, doi: 10.1109/TIP.2016.2639450.

[25] F. Liu, Z. Hua, J. Li, and L. Fan, "Low-light image enhancement network based on recursive network," (in English), *Frontiers Neurorobotics*, vol. 16, Mar. 2022, Art. no. 836551, doi: 10.3389/fnbot.2022.836551.

[26] X. Ren, W. Yang, W.-H. Cheng, and J. Liu, "LR3M: Robust low-light enhancement via low-rank regularized Retinex model," *IEEE Trans. Image Process.*, vol. 29, pp. 5862–5876, 2020, doi: 10.1109/TIP.2020.2984098.

[27] P. Qu, Z. Tian, L. Zhou, J. Li, G. Li, and C. Zhao, "SCDNet: Self-calibrating depth network with soft-edge reconstruction for low-light image enhancement," *Sustainability*, vol. 15, no. 2, p. 1029, Jan. 2023, doi: 10.3390/su15021029.

[28] E. H. Land, "The Retinex," *Amer. Sci.*, vol. 52, no. 2, pp. 247–264, 1964.

[29] C.-H. Lee, J.-L. Shih, C.-C. Lien, and C.-C. Han, "Adaptive multiscale Retinex for image contrast enhancement," in *Proc. Int. Conf. Signal-Image Technol. Internet-Based Syst.*, Dec. 2013, pp. 43–50, doi: 10.1109/SITIS.2013.19.

[30] W. Kim, "Low-light image enhancement: A comparative review and prospects," *IEEE Access*, vol. 10, pp. 84535–84557, 2022, doi: 10.1109/ACCESS.2022.3197629.

[31] S.-C. Huang, F.-C. Cheng, and Y.-S. Chiu, "Efficient contrast enhancement using adaptive gamma correction with weighting distribution," *IEEE Trans. Image Process.*, vol. 22, no. 3, pp. 1032–1041, Mar. 2013, doi: 10.1109/TIP.2012.2226047.
[32] P. Musa, F. A. Rafi, and M. Lamsani, "A review: Contrast-limited adaptive histogram equalization (CLAHE) methods to help the application of face recognition," in *Proc. 3rd Int. Conf. Informat. Comput. (ICIC)*, Oct. 2018, pp. 1–6, doi: 10.1109/IAC.2018.8780492.
[33] X. Guo and Q. Hu, "Low-light image enhancement via breaking down the darkness," *Int. J. Comput. Vis.*, vol. 131, no. 1, pp. 48–66, Jan. 2023, doi: 10.1007/s11263-022-01667-9.
[34] A. Punnappurath, A. Abuolaim, A. Abdelhamed, A. Levinshtein, and M. S. Brown, "Day-to-night image synthesis for training nighttime neural ISPs," in *Proc. IEEE/CVF Conf. Comput. Vis. Pattern Recognit. (CVPR)*, Jun. 2022, pp. 10759–10768.
[35] D. Varga, "Full-reference image quality assessment based on an optimal linear combination of quality measures selected by simulated annealing," *J. Imag.*, vol. 8, no. 8, p. 224, Aug. 2022.
[36] D. Varga, "No-reference image quality assessment with convolutional neural networks and decision fusion," *Appl. Sci.*, vol. 12, no. 1, p. 101, Dec. 2021.
[37] A. Mittal, R. Soundararajan, and A. C. Bovik, "Making a 'completely blind' image quality analyzer," *IEEE Signal Process. Lett.*, vol. 20, no. 3, pp. 209–212, Mar. 2013, doi: 10.1109/LSP.2012.2227726.
[38] D. R. I. M. Setiadi, "PSNR vs SSIM: Imperceptibility quality assessment for image steganography," *Multimedia Tools Appl.*, vol. 80, no. 6, pp. 8423–8444, Mar. 2021, doi: 10.1007/s11042-020-10035-z.
[39] Z. Wang, E. P. Simoncelli, and A. C. Bovik, "Multiscale structural similarity for image quality assessment," in *Proc. 37th Asilomar Conf. Signals, Syst. Comput.*, Nov. 2003, pp. 1398–1402, doi: 10.1109/ACSSC.2003.1292216.
[40] Y. Gao, X. Min, Y. Zhu, J. Li, X.-P. Zhang, and G. Zhai, "Image quality assessment: From mean opinion score to opinion score distribution," in *Proc. 30th ACM Int. Conf. Multimedia*, Lisboa, Portugal, Oct. 2022, pp. 997–1005, doi: 10.1145/3503161.3547872.

THAWEESAK TRONGTIRAKUL received the B.E. degree in electrical power engineering from the Rajamangala University of Technology Phra Nakhon (RMUTP), the M.Eng. degree in instrumentation engineering from the King Mongkut's Institute of Technology Ladkrabang (KMITL), and the D.Eng. degree in electronics and telecommunication from the King Mongkut's University of Technology Thonburi (KMUTT), Bangkok, Thailand. Currently, he is with the Electrical Engineering Department, Faculty of Industrial Education, RMUTP. Prior to his tenure with RMUTP, he was a Visiting Scientist with the College of Staten Island (CSI), and the Graduate Center, The City University of New York (CUNY). His research interests include the development of multi-model algorithms for simulation, signal processing, image processing, and video processing.

SOS S. AGAIAN (Life Fellow, IEEE) is a Distinguished Professor with the College of Staten Island (CSI), The City University of New York. The technologies he invented have been adopted by multiple institutions, including the U.S. Government and commercialized by industry. He has authored over 800 technical articles and ten books in his research areas. He is also listed as a co-inventor on 54 patents/disclosures. He gave over 30 plenary/keynote speeches and over 80 invited talks. His current research focuses on computational vision, artificial intelligence, multimedia security, multimedia analytics, and biologically inspired signal/image processing modeling. He is a fellow of SPIE, IS&T, AAAS, and AAIA. He received the Distinguished Research Award from The University of Texas at San Antonio, the Innovator of the Year Award, in 2014, and the Tech Flash Titans-Top Researcher Award (*San Antonio Business Journal*). He also received several best paper awards. He is the co-founder of three university centers. He is an Associate Editor of IEEE TRANSACTIONS ON IMAGE PROCESSING, IEEE TRANSACTIONS ON SYSTEMS, MAN, AND CYBERNETICS, and the *Journal of Electronic Imaging* (IS&T and SPIE).

SHIQIAN WU (Senior Member, IEEE) received the B.Eng. and M.Eng. degrees from the Huazhong University of Science and Technology (HUST), Wuhan, China, in 1985 and 1988, respectively, and the Ph.D. degree from Nanyang Technological University, Singapore, in 2001. He is currently a Professor with the School of Information Science and Engineering, Institute of Robotics and Intelligent Systems, Wuhan University of Science and Technology; and the Director of the Hubei Province Key Laboratory, Intelligent Information Processing and Real-Time Industrial Systems, Wuhan. He was an Assistant Professor, a Lecturer, and an Associate Professor with HUST, from 1988 to 1997. From 2000 to 2014, he was a Research Fellow or a Research Scientist with the Agency for Science, Technology and Research, Singapore. He has authored or coauthored two books and over 220 scientific publications (book chapters and journal/conference papers). His current research interests include image processing, pattern recognition, machine vision, and artificial intelligence.